Stimulated raman adiabatic passage in optomechanics
Fedoseev, V.

4 Quantum state transfer and entanlement via STIRAP

In this chapter we show the feasibility of preparing a single-phonon mechanical Fock state in mechanical mode 1 and transferring this state to mechanical mode 2 using optomechanical STIRAP and reading out the final state with current technology. Also we discuss modifications to STIRAP allowing to entangle mechanical states and verify an entangled state.

This chapter is partially based on Supplemental Material of: **V. Fedoseev**, F. Luna, I. Hedgepeth, W. Löffler and D. Bouwmeester, Stimulated Raman Adiabatic Passage in Optomechanics, Phys. Rev. Lett. 126, 113601 (2021). Simulations of this chapter were done together with Ian Hedgepeth.

4.1 STIRAP of a single phonon state

4.1.1 Introduction

STIRAP technique was initially developed to manipulate quantum states. Here we show that optomechanical STIRAP can be used to manipulate quantum states of mechanical modes. State transfer via STIRAP of single-phonon Fock state can in principle be observed experimentally with the same membranes in a cryogenic setting. Specifically, we consider 2 defect modes of the membranes discussed before. We provide a full quantum treatment of the protocol for such a state transfer including known sources of noise and unwanted effects: thermalization to the environment, heating by the laser light fields, the presence of other nearby membrane modes, realistic overall detection efficiency and dark count rate of a single photon detector. We consider STIRAP between two modes of the defect of the phononic crystal in the membrane, with quality factors of 10^9 [63] (we observed 0.25×10^9 for one of our membranes at 1 K), resulting in a thermal decoherence time [9] of approximately 5 ms at 1 K (1 phonon is added from the environment). This sets the time scale for the whole experiment. In laser cooling experiments [64, 65] the steady state temperature of similar membranes was observed to be less than 0.5 K above the cryostat base temperature when being sideband cooled, thus we adopt 1 K as a conservative estimate for the membrane temperature due to laser heating when operating in a dilution cryostat.

We assume the system to be at 1 K at all times for simplicity. The protocol consists of the following steps: both modes are sideband cooled to an average phonon occupation $\bar{n} = 0.1$, which is a reasonable assumption [64, 66, 67] and requires $g/\kappa \sim 0.03$ for our membranes, where g is the multiphoton optomechanical coupling, κ is the cavity linewidth; detection of a Stokes photon from a weak blue-detuned pulse projects the state of mode 1 to a state close to single-phonon Fock state; the STIRAP pulse sequence is sent; the state of the modes is read-out by a strong red-detuned pulse through detection of anti-Stokes photons. It is essential to filter out the strong pump light fields and to send the scattered photons to a single photon detector with high enough overall detection efficiency. Based on demonstrated experimental parameters we calculate that single-phonon Fock state can be transferred with fidelity of 60%.

We assume the following parameters of the system: mechanical mode 1 with resonance frequency $\omega_1/2\pi = 1.2$ MHz and quality factor $Q = 10^9$, single-photon optomechanical coupling $g_{01}/2\pi = 1$ Hz; mechanical mode 2 with resonance frequency $\omega_2/2\pi = 1.4$ MHz and quality factor $Q = 10^9$, single photon optomechanical coupling $g_{02}/2\pi = 1$ Hz; cavity linewidth $\kappa/2\pi = 50$ kHz and environment temperature $T = 1$ K. Such a high quality factor in membranes can be observed only for mechanical modes of a defect in the phononic crystal. Thus we are limited to the modes from the phononic bandgap typically having the width of 300 kHz. To minimize the crosstalk between mechanical mode 1 and mechanical mode 2, their resonances should be separated in frequency as much as possible, there should be no other modes in the vicinity of ~ 50 kHz. This defines our choice for ω_1 and ω_2.

The system evolution consisting of mechanical mode 1, mechanical mode 2 and the optical mode (all scattered photons) is calculated using Quantum Toolbox in Python (QuTiP) [68] during all the whole protocol. In the presence of N pump light fields α_i with detuning $\Delta_i = \omega_{\mathrm{L}i} - \omega_{\mathrm{cav}}$ the interaction part of the Hamiltonian reads as follows:

$$H_{\mathrm{int}} = \sum_{i=1}^{N} \sum_{j=1}^{2} g_{0j} \alpha_i (\hat{a}^\dagger e^{i\Delta_i t} + \hat{a} e^{-i\Delta_i t})(\hat{b}_j e^{-i\omega_j t} + \hat{b}_j^\dagger e^{i\omega_j t}) \tag{4.1}$$

in the triply rotating frame with mechanical frequencies and at ω_{cav}. We operate QuTiP in the density matrix formalism. The evolution of the full density matrix (mechanical mode 1, mechanical mode 2, the optical mode) is obtained via solving the Linblad equation:

$$\dot{\rho}(t) = \frac{-i}{\hbar} [H_{\mathrm{int}}, \rho] + \frac{\kappa}{2} \mathcal{L}(\hat{a}) + \sum_{i=1}^{2} \frac{\Gamma_{mi}}{2} \Big((\bar{n}_i + 1) \mathcal{L}(\hat{b}_i) + \bar{n}_i \mathcal{L}(\hat{b}_i^\dagger) \Big), \tag{4.2}$$

where $\mathcal{L}(\hat{O}) = \frac{1}{2}(2\hat{O}\rho(t)\hat{O}^\dagger - \rho(t)\hat{O}^\dagger\hat{O} - \hat{O}^\dagger\hat{O}\rho(t))$ are superoperators and $\bar{n}_i = (e^{\hbar\omega_i/k_b T} - 1)^{-1}$ is the average number of thermal phonons at the i-th mechanical frequency at the environment temperature T.

4.1.2 State preparation

We start from a thermal state of the mechanical modes corresponding to $T = 1$ K (about 10^4 phonons). Further, red-detuned pump light fields are sent to the cavity providing sideband cooling for each mechanical mode. We would like to note that sending two such light fields simultaneously looks very close to the STIRAP pulses (for the light frequency, not in the time domain). This might set the system in the dark mechanical state and prevent the loss of the mechanical population. To avoid this one of the light fields can be shifted in frequency by ~ 1 kHz from $\Delta_i = -\omega_i$, this will effectively destroy the mechanical dark state due to high 2-photon detuning.

In theory one can expect to reach $\bar{n}_{\min} = 10^{-4}$ for $g_r \sim \kappa$, but as the minimal reported thermal occupation is ~ 0.1 we restrict ourselves to $g_r/2\pi = 1600$ Hz resulting in the thermal state with $\bar{n} = 0.1$. This corresponds to a thermal state with

$$\begin{aligned}\rho_1^r =&0.906\,|0\rangle\,\langle 0| + 0.085\,|1\rangle\,\langle 1| + 0.008\,|2\rangle\,\langle 2| + \dots,\\ \rho_2^r =&0.906\,|0\rangle\,\langle 0| + 0.085\,|1\rangle\,\langle 1| + 0.008\,|2\rangle\,\langle 2| + \dots,\end{aligned} \tag{4.3}$$

where ρ_i^r is the reduced density matrix for mechanical mode i in the Fock basis.

Now mechanical mode 1 is prepared in a single-phonon state. For this a 0.1 ms blue-detuned pulse with $\Delta = \omega_1$ and $g^b/2\pi = 2410$ Hz is sent. This pulse increases the average occupation of the modes to $\bar{n}_1 = 0.20$ and $\bar{n}_2 = 0.12$ with the density matrices for modes 1 and 2:

$$\begin{aligned}\rho_1^b =&0.831\,|0\rangle\,\langle 0| + 0.140\,|1\rangle\,\langle 1| + 0.024\,|2\rangle\,\langle 2| + \dots,\\ \rho_2^b =&0.893\,|0\rangle\,\langle 0| + 0.095\,|1\rangle\,\langle 1| + 0.010\,|2\rangle\,\langle 2| + \dots.\end{aligned} \tag{4.4}$$

The pulse is weak, so that the probability of photon scattering in the cavity $p = 0.1$. Thus one time out of ten pulses a scattering event occurs and a Stokes photon is detected by the single photon detector (SPD). Such detection projects mechanical mode 1 state to a non-classical state:

$$\rho_1^{her} = 0.831\,|1\rangle\,\langle 1| + 0.140\,|2\rangle\,\langle 2| + 0.024\,|3\rangle\,\langle 3| + \dots. \tag{4.5}$$

Just after the detection there is no vacuum component in mechanical mode 1 and its state is close to single-phonon state.

Detection of a scattered photon requires filtering of the pump light fields. Such a filter was demonstrated in [66] with pump light attenuation of 150 dB at a cost of 30% transmission for the light frequency of interest. Overall detection efficiency was reported 2.5% with avalanche SPD having detection efficiency of 30%.

In reality SPDs always have non-zero dark count rate (DCR), clicking of the detector due to DCR admixes thermal state ρ_1^b to the projected state of mechanical mode 1. Let's take this into account. A conservative estimate of DCR is 10 Hz, though our superconducting nanowire SPD (SNSPD) achieve DCR of 0.01 Hz with proper stray light isolation. Thus keeping in mind SNSPD with detection efficiency of 90% further we assume overall detection efficiency $\eta = 0.075$. The rate of detected Stokes photons is $(\tau_b/p\eta)^{-1} = 75$ Hz, thus the density matrix of mode 1 after a click of the detector is

$$\begin{aligned}\rho_1^i &= \frac{10 \text{ Hz}}{10 \text{ Hz} + 75 \text{ Hz}}\rho_1^b + \frac{75 \text{ Hz}}{10 \text{ Hz} + 75 \text{ Hz}}\rho_1^{her} = \\ &= 0.098 \left|0\right\rangle \left\langle 0\right| + 0.750 \left|1\right\rangle \left\langle 1\right| + 0.126 \left|2\right\rangle \left\langle 2\right| + \dots .\end{aligned} \tag{4.6}$$

Detection of the Stokes photon practically does not change the state of mode 2.

4.1.3 STIRAP

The previous steps are repeated until a click of the SPD. Just after the click the STIRAP pulse sequence $\alpha_1(t)$ and $\alpha_2(t)$ is sent, where

$$\begin{aligned}\alpha_1(t) &= \alpha_{max} e^{-(t-\tau)^2/2\sigma^2} \\ \alpha_2(t) &= \alpha_{max} e^{-(t+\tau)^2/2\sigma^2}\end{aligned} \tag{4.7}$$

and $\sigma = 0.14$ ms, $\tau = \sigma/3$, $\alpha_{max} = 5000$. Simulation of these pulses with the initial state ρ_1^i and ρ_2^b produces Fig. 4.1. The resulting states of the mechanical modes after the pulses are

$$\begin{aligned}\rho_1^s &= 0.900 \left|0\right\rangle \left\langle 0\right| + 0.091 \left|1\right\rangle \left\langle 1\right| + 0.007 \left|2\right\rangle \left\langle 2\right| + \dots , \\ \rho_2^s &= 0.370 \left|0\right\rangle \left\langle 0\right| + 0.447 \left|1\right\rangle \left\langle 1\right| + 0.137 \left|2\right\rangle \left\langle 2\right| + \dots .\end{aligned} \tag{4.8}$$

Mode 1 is in a state very close to the initial thermal state ρ_1^r. The single phonon transfer efficiency is $0.447/0.75 = 0.596$.

Note that for this calculation the scattered photons at ω_{cav} are not monitored. In the hypothetical case of very high total detection efficiency $\eta \sim 1$ the state transfer fidelity can be increased to near unity: if the heralding photon during the STIRAP pulses is detected, then the quantum state of mechanical mode 1 is lost to the optical mode and the whole experiment should be repeated until no such heralded photon is detected.

Low temperature of the environment is essential for this experiment. We simulated the transfer at $T = 8$ K, the results are shown in Fig. 4.2. In this case thermalization to environment is 8 times faster, and STIRAP with high transfer efficiency would require higher than available pump intensity (due to weak coupling requirement). With $\alpha = 5000$ the evolution of probability of mode 2 being in single phonon state is similar to just thermalization to the environment without the STIRAP pulses.

4.1.4 Readout

The final state of the mechanical modes is read out with a strong red-detuned pulse with $g/2\pi = 5000$ Hz and duration of 0.5 ms (each mode requires separate read out with appropriate detuning $\Delta = -\omega_i$). Such a pulse provides a scattering probability of 99.8% and thus if the mechanical mode is not in the vacuum state, this pulse

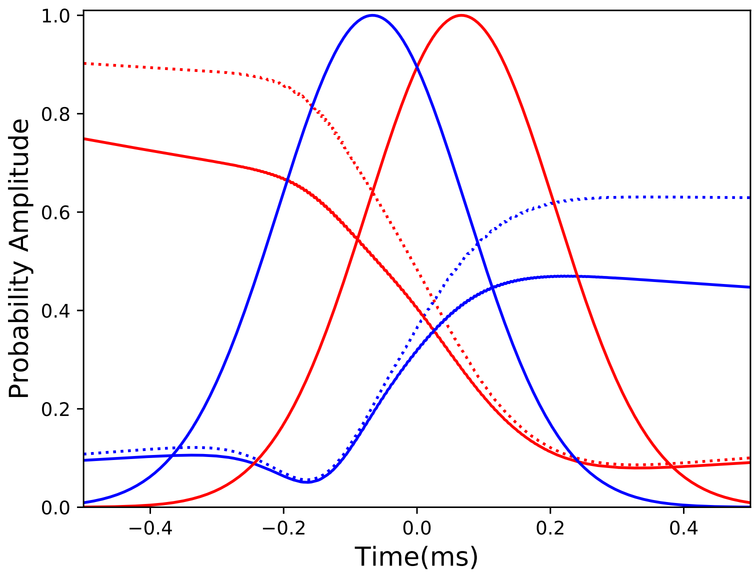

Figure 4.1: State transfer using STIRAP at 1K. Red and blue represent the first and second modes respectively. Solid denotes the probability of detecting a single phonon (ρ_{11}), while dotted denotes the probability that the mode is populated ($1-\rho_{00}$). The efficiency of state transfer is 59.6% and includes unmatched sidebands.

produces an anti-Stokes photon (or photons). We assume that the SNSPD is not photon number resolving, meaning that absorption of a two photon state results in the same click as a single photon. So we cannot distinguish between a single phonon and more than 1 phonon state of a mechanical mode. Thus what we can observe is $1-\rho_{00}$ rather than ρ_{11}. This probability is plotted in Fig. 4.1 by dashed line. Knowledge of the total detection efficiency η and DCR of our detector allows to estimate $1-\rho_{00}$ term of both mechanical modes.

4.1.5 Discussion

The whole experiment looks as follows:
1) both modes are sideband-cooled during 5 ms;
2) the blue-detuned pulse is sent. If the heralded photon is detected, we proceed to step 3), otherwise repeat 1) and 2);
3) the STIRAP pulse sequence is sent;
4) the red-detuned readout pulse is sent to get information about mechanical mode i, $i = 1$ or 2.

Let's calculate the time to get a single anti-Stokes photon detection at step 4). To

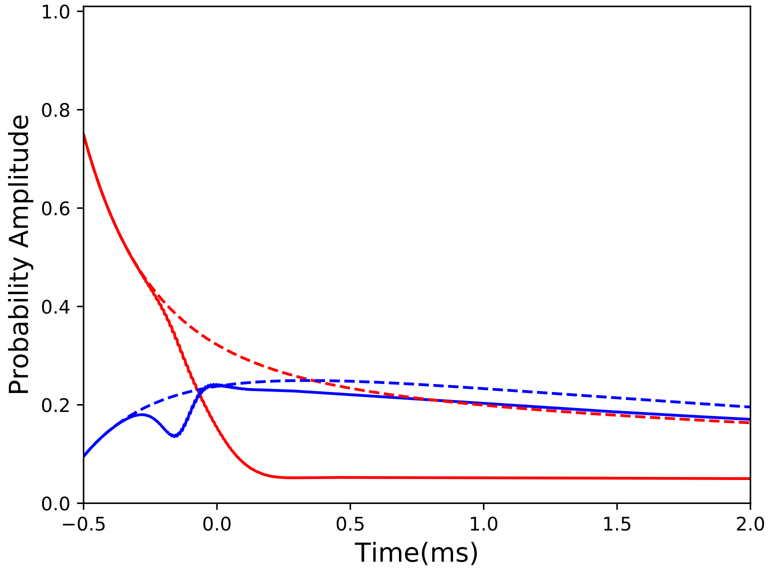

Figure 4.2: State transfer at 8K realized using STIRAP. Red and blue represent the first and second modes respectively. Solid denotes a state transfer via STIRAP, while dashed denotes evolution in the presence of the environment, without the STIRAP pulses.

get to step 3) it will take on average

$$T_3 = \frac{5\text{ ms} + 0.1\text{ ms}}{0.1\eta} = 0.7\text{ s}. \tag{4.9}$$

The probability to detect a single anti-Stokes photon at step 4) is

$$P_f = \eta(1 - \rho_{00}) < 0.075. \tag{4.10}$$

Thus the time to get a single anti-Stokes photon detection at step 4) is $\frac{T_3}{P_f} > 9.3$ s. Now, let's estimate the effect of DCR of 10 Hz. The detection rate of the heralding Stokes photon from 2) is 75 Hz. At this stage our single-phonon state preparation deteriorates, but not significantly, see above. During the detection of herading anti-Stokes photon from step 4) the signal rate is

$$f_4 = (\frac{0.5\text{ ms}}{P_f})^{-1} = 150\text{ Hz (for } 1 - \rho_{00} = 1). \tag{4.11}$$

At step 4) DCR should be subtracted from the clicking rate. DCR equals the photon detection rate for $1 - \rho_{00} = 0.07$. We can conclude that DCR of 10 Hz is not a limiting factor for the considered parameters of the experiment.

4.1.6 Other Membrane Modes

Now we consider the presence of other nearby mechanical modes in the membrane. The STIRAP protocol relies on the heralding Stokes photons from the blue-detuned pulse and anti-Stokes photons from the read-out pulse. These two pulses affect other modes of the membrane in the frequency range of a few κ around ω_1 and ω_2. As a consequence, a flux of spurious Stokes and anti-Stokes photons is produced by these modes. We have observed modes in our membranes with quality factors as low as 10^6 in the vicinity of mode 1 and 2. The upper bound of the rate for the phonons to enter these modes from the environment is 100 kHz (based on $\Phi \approx \Gamma_m n_{th}$ where $n_{th} = 10^5$). Additionally, the upper limit for the conversion of phonons into photons for these modes is $\Gamma_{opt}/2\pi$ <2 kHz.

Because we are operating in the bandgap of our membrane, the spurious modes are at least 70 kHz away from modes 1 and 2. This is also the minimal frequency separation of the spurious photons from ω_{cav}, where the heralded photons are passing through the cascade of filtering cavities described above. These filtering cavities produce at least 50 dB of isolation at 70 kHz [66] detuning, which decreases the flux of the spurious photons factor of 10^5 not taking into account the detection efficiency. This causes the rate of detector clicks due to other modes in the membrane to become negligibly small and does not effect the STIRAP protocol.

4.1.7 Conclusions

We discussed and estimated quantitatively a protocol where two mechanical modes of our membrane are cooled near a quantum ground state, mode 1 is prepared in a close to single-phonon Fock state and this state is transferred to mechanical mode 2 of the same membrane. We used conservative parameters of the whole experiment and showed that it is feasible to observe such a state transfer with state of the art membrane-in-the-middle sideband-resolved system. We included in our consideration all known experimental complications. The main challenge of the experiment is to keep heating of the membrane due to pump light fields at a level that the temperature of the membrane is below 1 K. This requirement appears to keep the rate of thermalization to environment at an acceptable level.

4.2 Creation and detection of an entangled state

In [69] it was shown that the STIRAP pulse sequence can be modified to produce a system in a superposition of two quantum states. Let's consider the dark state which the system is following during STIRAP:

$$\Phi_0(t) = \cos\theta(t)\psi_1 - \sin\theta(t)\psi_3, \tag{4.12}$$

with $\tan\theta(t) = \Omega_{12}(t)/\Omega_{23}(t)$, where $\Omega_{ij}(t)$ is the Rabi frequency of the coupling between states i and j. In STIRAP we start from the system being in state ψ_1 requiring $\Omega_{12}(t=-\infty)/\Omega_{23}(t=-\infty) = 0$ and finish in state ψ_3 requiring $\Omega_{23}(t=\infty)/\Omega_{12}(t=\infty) = 0$, see Fig. 4.3. If the pulses are modified such that they start as in STIRAP and finish with constant ratio of drive strength $\Omega_{12}(t)/\Omega_{23}(t) = \mathrm{const} = r$, see Fig. 4.4, then the system ends up in a superposition state

$$\Phi_{\text{final}} = \alpha\psi_1 - \beta\psi_3, \tag{4.13}$$

where $\alpha = 1/\sqrt{1+r^2}$ and $\beta = r/\sqrt{1+r^2}$. Indeed, at the time when the ratio of the driving strengths approaches r (dashed line Fig. 4.4) the system reaches state Φ_{final}, and at all times after this moment the system stays in Φ_{final} including the time when the pulses are finished.

In optomechanical STIRAP such modified pulses with $r = 1$ will produce an entangled state of the mechanical modes:

$$\Phi_{\text{final}} = (|1\rangle_1 |0\rangle_2 - |0\rangle_1 |1\rangle_2)/\sqrt{2}, \tag{4.14}$$

where $|n\rangle_i$ is mechanical mode i in n-phonon Fock state. All simulations of this section are done with the following parameters: $\omega_1/2\pi = 1.2$ MHz, $\omega_2/2\pi = 1.4$ MHz, $Q = 10^9$, $\kappa/2\pi = 50$ kHz, $g_{\max}/2\pi = 5$ kHz, $T = 0$. These parameters satisfy the criterion of adiabaticity and are chosen to show the properties of fractional STIRAP in a clear way. Note, the optical mode (green dashed line) is practically not populated in line with the adiabatic evolution.

Due to time reversal symmetry this process can be reversed: we start from a superposition $(|1\rangle_1 |0\rangle_2 - |0\rangle_1 |1\rangle_2)/\sqrt{2}$ and after the pulses have been sent mode 1 reaches single-phonon state, mode 2 reaches vacuum state, see Fig. 4.5. The optical mode is also practically not occupied in this process.

But if the initial state of the system differs from Eq. 4.14, then this state is also different from the dark state dictated by the ratio of the drive strengths. Thus the quantum state of the system will evolve to reach this dark state. For example, if the initial state of the system is $(|1\rangle_1 |0\rangle_2 + |0\rangle_1 |1\rangle_2)/\sqrt{2}$, then the optical mode becomes populated during the pulses, see Fig. 4.6. By the time system reaches the dark state (approximately -0.8 ms) all the population is lost to the optical mode and the final state is vacuum for both mechanical modes.

For any other initial state different from $(|1\rangle_1 |0\rangle_2 + |0\rangle_1 |1\rangle_2)/\sqrt{2}$ the final state will not be vacuum. For example, if the initial state is a classical mixture

$$\rho = (|1\rangle_1 |0\rangle_2 \langle 0|_2 \langle 1|_1 + |0\rangle_1 |1\rangle_2 \langle 1|_2 \langle 0|_1)/2, \tag{4.15}$$

then the final state is $\rho_1 = 0.5\left|0\right\rangle\left\langle 0\right| + 0.5\left|1\right\rangle\left\langle 1\right|$ and mode 2 is in the vacuum state, see Fig. 4.7. The system reaches the dark state at approximately -0.8 ms loosing half of the initial population to the optical mode and then the system follows the dark state according to the driving pulses without further loss.

These properties of reversed fractional STIRAP open a way to probe the quantum

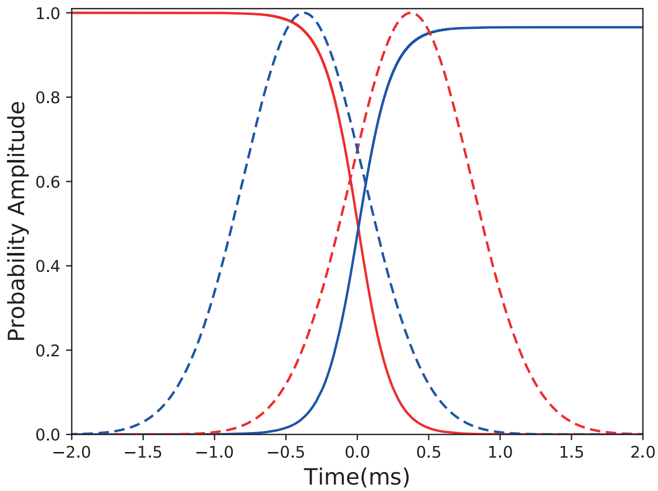

Figure 4.3: State transfer using STIRAP at $T = 0$. Red and blue represent mechanical mode 1 and mechanical mode 2 respectively. Solid lines denote the probability of a single Fock state ρ_{11}, while dashed lines denote the pulses driving strength Ω_{12} and Ω_{23}.

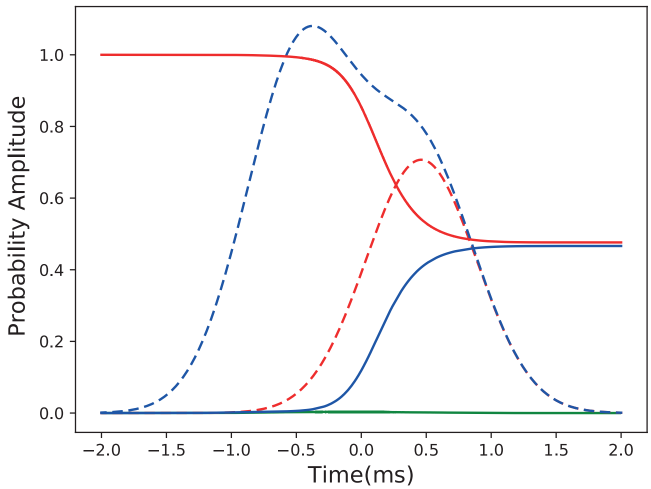

Figure 4.4: Creation of mechanical modes entanglement $(\left|1\right\rangle_1\left|0\right\rangle_2 - \left|0\right\rangle_1\left|1\right\rangle_2)/\sqrt{2}$ using fractional STIRAP at $T = 0$. Red, blue and green represent mechanical mode 1, mechanical mode 2 and the optical mode respectively. Solid lines denote the probability of a single Fock state ρ_{11}, while dashed lines denote the pulses driving strength Ω_{12} and Ω_{23}.

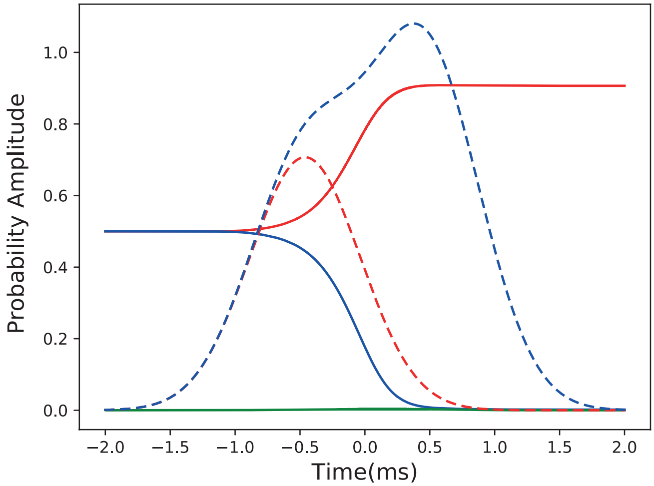

Figure 4.5: Reverse fractional STIRAP: entanglement verification, initial state $(|1\rangle_1 |0\rangle_2 - |0\rangle_1 |1\rangle_2)/\sqrt{2}$. Mode 1 ends up in single-phonon state. Red, blue and green represent mechanical mode 1, mechanical mode 2 and the optical mode respectively. Solid lines denote the probability of a single Fock state ρ_{11}, while dashed lines denote the pulses driving strength Ω_{12} and Ω_{23}.

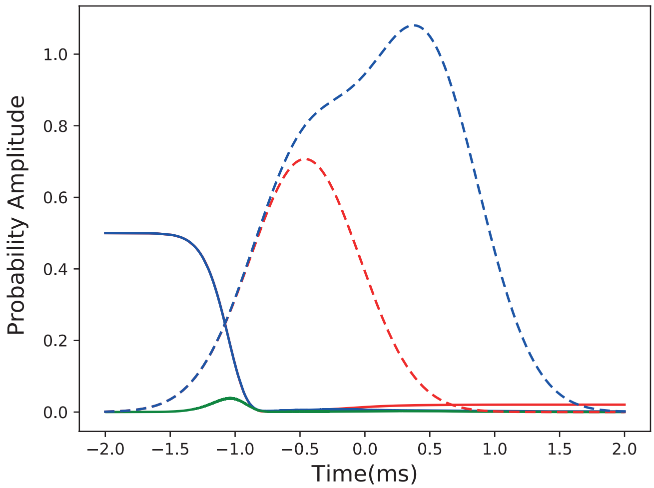

Figure 4.6: Reverse fractional STIRAP: entanglement verification, initial state $(|1\rangle_1 |0\rangle_2 + |0\rangle_1 |1\rangle_2)/\sqrt{2}$. Both mechanical modes end up in vacuum state. Red, blue and green represent mechanical mode 1, mechanical mode 2 and the optical mode respectively. Solid lines denote the probability of a single Fock state ρ_{11}, while dashed lines denote the pulses driving strength Ω_{12} and Ω_{23}. Note, the loss occurs via population of the optical mode.

state of a multimode optomechanical system as demonstrated by the three cases of different initial states. Thus this process can be used to differentiate between an

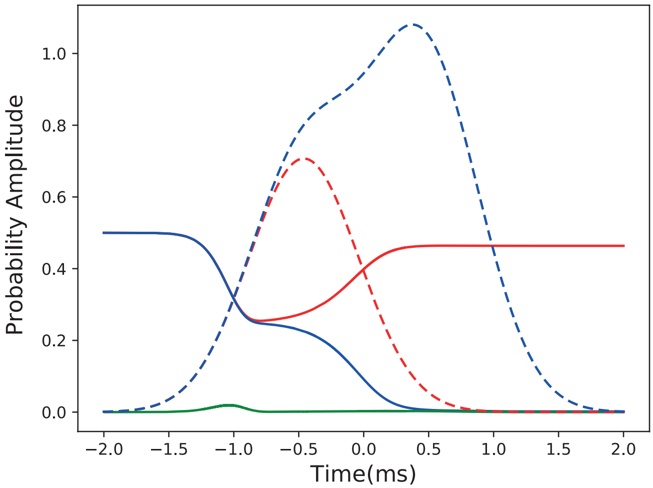

Figure 4.7: Reverse fractional STIRAP: entanglement verification, initial state is statistical mixture $\rho = (|1\rangle_1 |0\rangle_2 \langle 0|_2 \langle 1|_1 + |0\rangle_1 |1\rangle_2 \langle 1|_2 \langle 0|_1)/2$. Mode 1 ends up in approximately $\rho = 0.5\,|0\rangle\langle 0| + 0.5\,|1\rangle\langle 1|$. Red, blue and green represent mechanical mode 1, mechanical mode 2 and the optical mode respectively. Dashed lines denote the probability of a single Fock state ρ_{11}, while solid lines denote the pulses driving strength Ω_{12} and Ω_{23}. Note, the loss occurs via population of the optical mode.

entangled state and a classical statistical mixture.

Another application of STIRAP in optomechanics is testing whether extra channels of decoherence are present in the system. Dark mode evolution in STIRAP requires the presence of the off-diagonal terms in the full density matrix as can be seen from Eq. 4.12. If a particular model of decoherence requires fast decay of the off-diagonal terms, then during the STIRAP pulses all the population will be lost to the optical mode similar to the considered case shown in Fig. 4.6, and the final population will be vacuum for all the modes. Therefore, experimental STIRAP resulting in the vacuum state for a system where a non-vacuum final state is predicted by the theory might indicate the existence of extra decoherence channels.